



# The C-terminal domain of the MERS coronavirus M protein contains a *trans*-Golgi network localization signal

Received for publication, April 18, 2019, and in revised form, August 6, 2019. Published, Papers in Press, August 9, 2019, DOI 10.1074/jbc.RA119.008964

Anabelle Perrier<sup>1</sup>, Ariane Bonnin, Lowiese Desmarests<sup>2</sup>, Adeline Danneels, Anne Goffard, Yves Rouillé, Jean Dubuisson, and  Sandrine Belouzard<sup>3</sup>

From the Université Lille, CNRS, INSERM, CHU Lille, Institut Pasteur de Lille, U1019-UMR 8204-CILL-Center for Infection and Immunity of Lille, F-59000 Lille, France

Edited by Phyllis I. Hanson

Coronavirus M proteins represent the major protein component of the viral envelope. They play an essential role during viral assembly by interacting with all of the other structural proteins. Coronaviruses bud into the endoplasmic reticulum (ER)–Golgi intermediate compartment (ERGIC), but the mechanisms by which M proteins are transported from their site of synthesis, the ER, to the budding site remain poorly understood. Here, we investigated the intracellular trafficking of the Middle East respiratory syndrome coronavirus (MERS-CoV) M protein. Subcellular localization analyses revealed that the MERS-CoV M protein is retained intracellularly in the *trans*-Golgi network (TGN), and we identified two motifs in the distal part of the C-terminal domain as being important for this specific localization. We identified the first motif as a functional diacidic DxE ER export signal, because substituting Asp-211 and Glu-213 with alanine induced retention of the MERS-CoV M in the ER. The second motif, <sup>199</sup>KxGxYR<sup>204</sup>, was responsible for retaining the M protein in the TGN. Substitution of this motif resulted in MERS-CoV M leakage toward the plasma membrane. We further confirmed the role of <sup>199</sup>KxGxYR<sup>204</sup> as a TGN retention signal by using chimeras between MERS-CoV M and the M protein of infectious bronchitis virus (IBV). Our results indicated that the C-terminal domains of both proteins determine their specific localization, namely TGN and ERGIC/*cis*-Golgi for MERS-M and IBV-M, respectively. Our findings indicate that MERS-CoV M protein localizes to the TGN because of the combined presence of an ER export signal and a TGN retention motif.

Coronaviruses (CoVs)<sup>4</sup> are widespread pathogens that can infect a wide variety of species among mammals and birds (1, 2),

This work was supported by a Visionn-AIRR grant from Region Hauts-de-France. The authors declare that they have no conflicts of interest with the contents of this article.

<sup>1</sup> Supported by a fellowship from the University of Lille and the Region Hauts-de-France.

<sup>2</sup> Supported by a fellowship from the Region Hauts-de-France.

<sup>3</sup> To whom correspondence should be addressed. E-mail: sandrine.belouzard@ibl.cnrs.fr.

<sup>4</sup> The abbreviations used are: CoV, coronavirus; HCoV, human CoV; SARS, severe acute respiratory syndrome; MERS, Middle East respiratory syndrome; S, E, M, and N protein; spike, envelope, membrane, and nucleocapsid protein, respectively; MHV, murine hepatitis virus; IBV, infectious bronchitis virus; ER, endoplasmic reticulum; ERGIC, ER–Golgi intermediate compartment; TGN, *trans*-Golgi network; MPR, mannose 6-phosphate receptor; PCC, Pearson correlation coefficient; PNGase F, peptide:N-glycosidase F; EndoH, endoglycosidase H; COPI and COPII, coat protein complex

including humans, causing mostly respiratory and enteric symptoms. There are six known coronaviruses infecting humans. The first human coronaviruses, HCoV-229E and HCoV-OC43, were isolated in the 1960s from patients suffering from a common cold. Administration of these viruses to volunteers rapidly confirmed their harmless character. Therefore, research on coronaviruses had been mostly of veterinary interest, but this changed recently with the emergence of two highly pathogenic human coronaviruses causing severe pneumonia epidemics. First, the severe acute respiratory syndrome coronavirus (SARS-CoV) appeared in 2002, and then the Middle East respiratory syndrome coronavirus (MERS-CoV) appeared in 2012. Both viruses have a zoonotic origin, showing that this virus family is a reservoir of emerging pathogens, especially because of their high interspecies transmission (3).

Coronaviruses are enveloped positive single-stranded RNA viruses, with a very large genome of 25–30 kb, belonging to the Coronaviridae family in the Nidovirales order. The viral particle is composed of a lipid envelope in which at least three structural proteins are anchored: the *spike* protein (S), the *envelope* protein (E), and the *membrane* protein (M). Inside the particle, the viral RNA is associated with the *nucleocapsid* protein (N), forming a helical capsid. The S protein triggers viral entry by binding to the cellular receptor and mediating fusion of the viral envelope with the host cell membrane (4, 5). The E protein is a small protein with multiple roles during infection (6). The SARS-CoV E protein plays an important role in viral pathogenesis, and this role can be linked to the ion channel activity of the protein (7). The E protein is also involved in viral assembly, trafficking, and egress of virions, by promoting membrane curvature and viral fission and by inducing morphological changes of the compartments of the secretory pathway (8, 9).

The M protein is the most abundant protein of the envelope (10). Its length ranges from 217 to 230 amino acid residues in most coronaviruses, but it can go up to 270 residues in some coronaviruses (bottlenose dolphin coronavirus). It is a protein with three membrane-spanning hydrophobic segments, a small N-terminal domain located outside the virion (or inside the lumen of intracellular organelles), and a large C-terminal domain that makes up half of the protein, inside the virion (or in the cytoplasm of infected cells) (10). M proteins of some alpha-coronaviruses contain an additional hydrophobic segment that

I and II, respectively; HA, hemagglutinin; PFA, paraformaldehyde; pAb, polyclonal antibody; CRT, calreticulin.

functions as a signal peptide. The M protein is invariably glycosylated on its N-terminal domain. However, there are differences in the type of glycosylation. The murine hepatitis virus (MHV) and some other *Betacoronavirus* M proteins are O-glycosylated, whereas *Alpha-* and *Deltacoronavirus* M proteins are modified with N-linked sugars. The glycosylation is dispensable for virus assembly (11). The M protein is considered to be the motor of the assembly of viral particles because it is able to interact with all of the other structural proteins (12–14). Important M–M interactions have also been demonstrated during assembly (15, 16). For many coronaviruses, including the transmissible gastroenteritis virus, MHV, and IBV, the co-expression of M and E proteins in cells is sufficient to induce the production of virus-like particles (17–19), indicating that these proteins are essential and sufficient to the assembly step. Only for SARS-CoV, the nucleocapsid protein has been shown to be additionally required for the production of virus-like particles (20). EM observations have shown that coronaviruses bud inside the ER–Golgi intermediate compartment (ERGIC) (21, 22) and then travel through the Golgi. Although the assembly step of coronaviruses occurs in the ERGIC compartment, it has been shown for several coronaviruses that the M protein expressed alone in cells can go beyond the assembly site in the secretory pathway (21). However, the subcellular localization of the M protein varies between the different coronavirus species. Indeed, MHV M protein can reach the *trans*-Golgi network (TGN), whereas IBV-M protein is retained in the ERGIC and one or two cisternae of the *cis*-Golgi (21, 23, 24). The intracellular retention of IBV-M has been attributed to the first membrane-spanning segment and particularly to polar residues located within this domain (25, 26). For MHV, both the TM1 and the last 22 amino acids seem to be important determinants for the intracellular localization of the protein (27). The aim of this study was to investigate the subcellular localization of the MERS-M protein and to characterize the signals involved in its trafficking.

## Results

### MERS-CoV M localizes in the *trans*-Golgi network

The M protein is composed of a short N-terminal domain followed by three membrane-spanning segments and a long C-terminal domain (Fig. 1A). To analyze the intracellular trafficking of the MERS-CoV M protein, we transfected a vector expressing the MERS-CoV M protein with a HA tag fused at its N terminus (HA-MERS-M) in HeLa cells and compared the protein localization with different compartment markers using immunofluorescence and confocal microscopy (Fig. 1B). As observed in Fig. 1B, MERS-CoV M shows a good colocalization with TGN46 that localizes in the *trans*-Golgi network. We confirmed this colocalization by co-transfection of the M protein with the GFP fused to the transmembrane domain and cytosolic tail of the cation-independent mannose 6-phosphate receptor (GFP-CI-MPR). This reporter has been shown to be localized in the TGN in HeLa cells (28). The images were then analyzed using ImageJ to calculate the Pearson correlation coefficient (PCC) for each co-staining (Fig. 1C). The PCC measures the pixel-by-pixel covariance of the signal levels of two

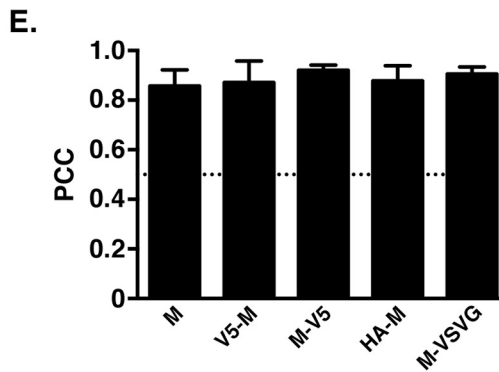
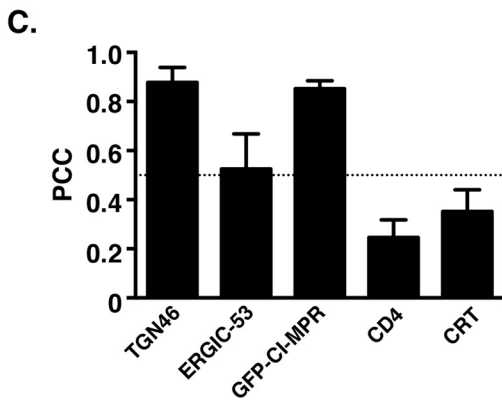
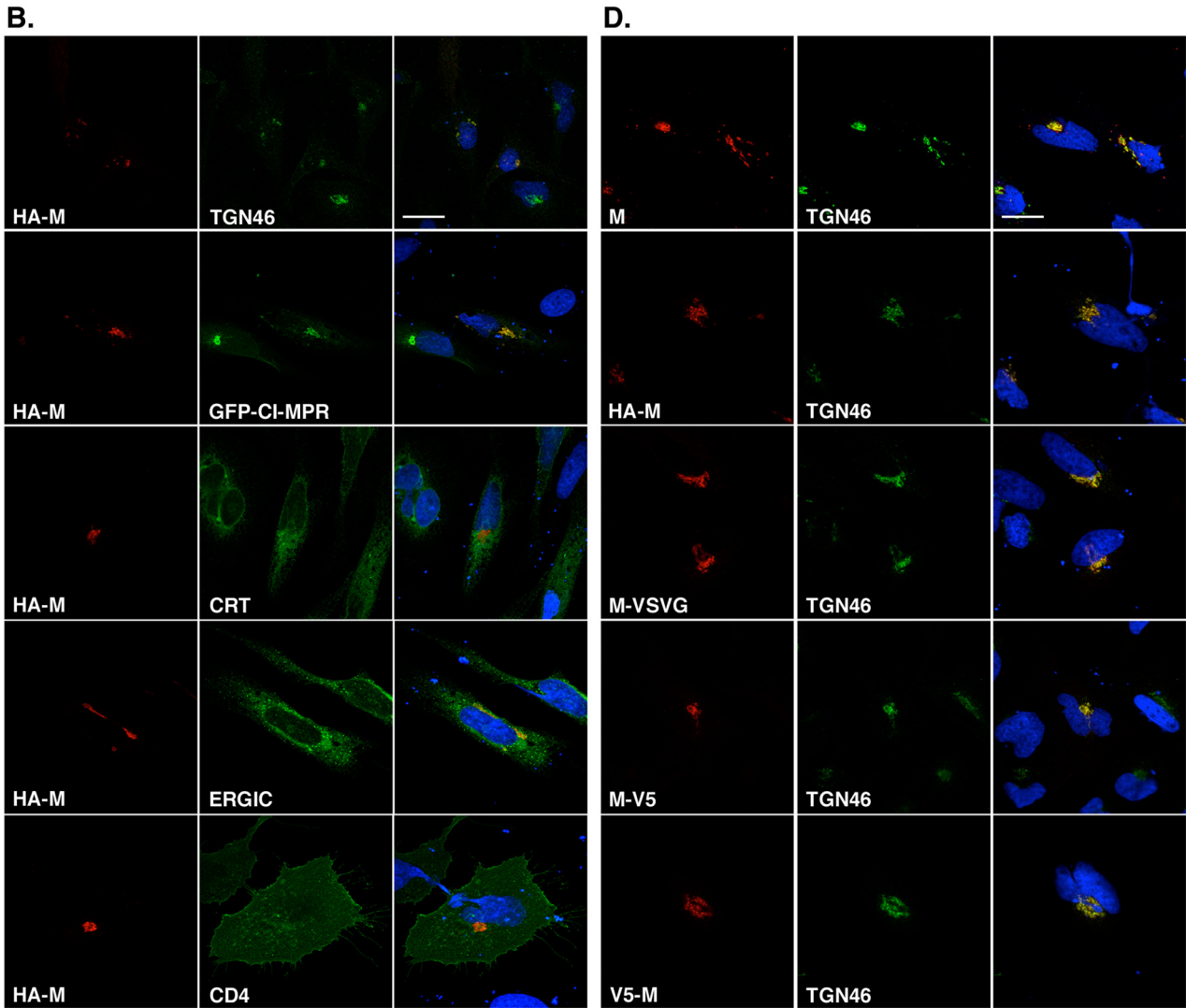
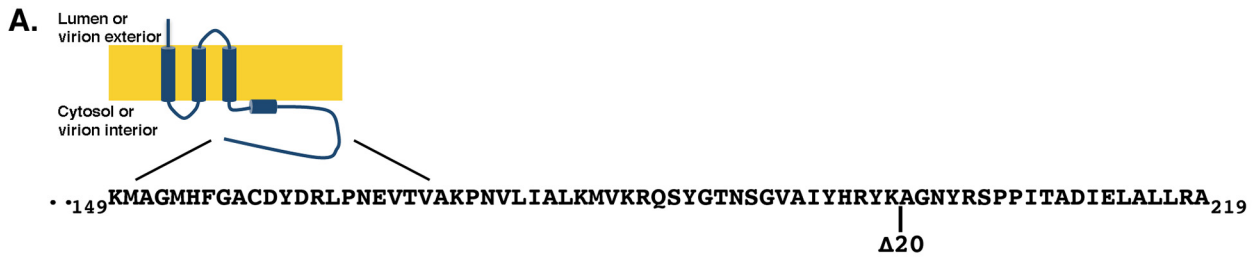
images (29). The PCC values range from  $-1$  to  $1$ . A PCC value of  $1$  is obtained for two images whose intensities of fluorescence are linearly and perfectly related, whereas a value of  $-1$  means that the intensities are inversely related to one another. Values near  $0$  mean that the intensities are uncorrelated. Our results confirm the localization of MERS-CoV M in the TGN with a PCC of  $0.878 (\pm 0.014)$  and  $0.852 (\pm 0.012)$  for the MERS-CoV M with TGN46 and GFP-CI-MPR markers, respectively. The PCCs for MERS-CoV M and CD4 (a cell surface marker) or the calreticulin (an ER marker) are below  $0.4$ . However, the PCC between MERS-CoV M and the ERGIC marker, ERGIC-53, is higher ( $0.524 \pm 0.03$ ).

To facilitate the detection of the M protein and particularly in co-staining experiments, different M protein constructs were generated with different tags either at the N terminus (HA or V5) or at the C terminus (V5 or VSVG). This offers the advantage of using a panel of antibodies raised in different species. To use these tools, we analyzed their intracellular localization to confirm that adding a tag, regardless of their sequence or the position of the insertion, had no effect on MERS-CoV M localization. We also generated a polyclonal antibody raised against a C-terminal peptide of the M protein to detect the untagged protein. This antibody was used to control the effect of the tags on the subcellular localization of the M protein. Cells expressing M or the different tagged versions of this protein were processed for double-label immunofluorescent detection of the M protein and TGN46 (Fig. 1D). For each protein, the colocalization level with the TGN46 marker was also quantified by calculating the PCC (Fig. 1E). As observed with HA-M, the untagged form of the protein presented a strong colocalization with the TGN46 marker (Fig. 1, D and E) with a PCC of  $0.857 \pm 0.015$ . Similar results were obtained with the other tagged proteins. Altogether, these results indicate that the MERS-CoV M protein expressed alone is located in the TGN and that the tag added to our constructs does not alter this localization.

### The last 20 residues of the C-terminal domain of the MERS-CoV M protein are important for the MERS-CoV M intracellular trafficking

To study the role of the C-terminal domain of MERS-CoV M in its intracellular trafficking, we constructed serial deletion mutants of 20 residues. The deletion of the last 20 residues of the MERS-CoV M protein ( $M\Delta 20$ ) produced mutants that were no longer localized in the TGN (Fig. 2A). Moreover, it induced a different intracellular localization, depending on the tag used. Indeed, HA- $M\Delta 20$  co-localizes with calreticulin, the ER marker, as shown by the double labeling in Fig. 2B, whereas  $M\Delta 20$ -VSVG was located at the cell surface, as shown by the double labeling of  $M\Delta 20$ -VSVG and CD4 (Fig. 2C). We measured the extent of colocalization for HA- $M\Delta 20$  or  $M\Delta 20$ -VSVG with the ER, TGN, or cell surface marker by measuring the PCC (Fig. 2D). The WT protein presented a PCC of  $0.905 \pm 0.007$  for TGN46 and of  $0.296 \pm 0.014$  and  $0.239 \pm 0.017$  for CRT and CD4, respectively. The HA- $M\Delta 20$  protein showed a decrease of the PCC for TGN46 ( $0.369 \pm 0.019$ ) associated with an increase of the PCC with CRT ( $0.855 \pm 0.011$ ). The HA- $M\Delta 20$  also showed a moderate increase in cell surface localization with a PCC for CD4 of  $0.539 \pm 0.018$ . The PCC

# MERS-CoV M protein TGN localization



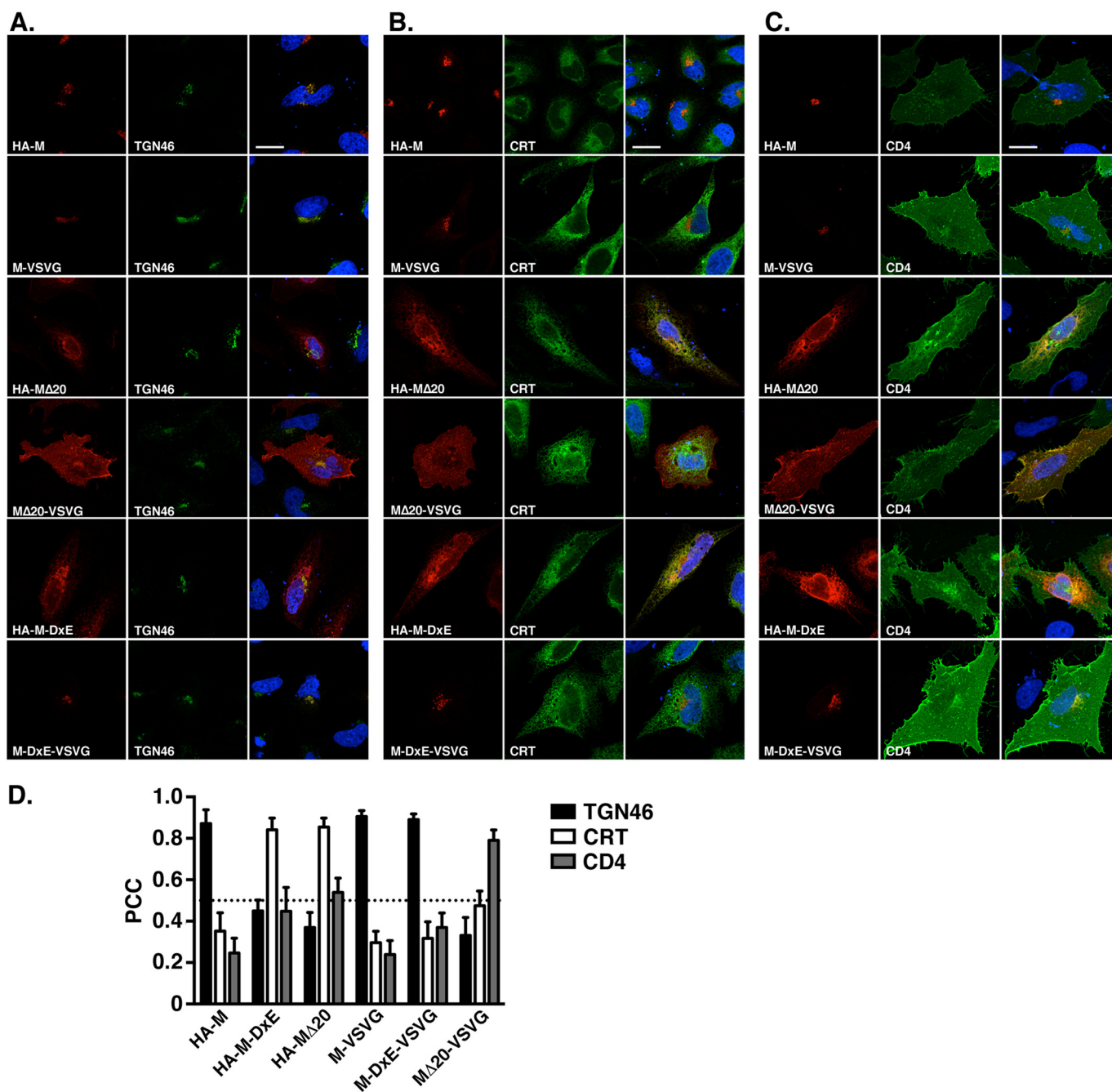


**Figure 2. The distal part of MERS-M C-terminal domain contains motif(s) involved in its subcellular localization.** Cells expressing the M protein (*HA-M* and *M-VSVG*) or the M protein lacking its last 20 residues (*HA-MΔ20* or *MΔ20-VSVG*) or the M protein with Asp-211 and Glu-213 mutated into Ala (*HA-M-DxE* or *M-DxE-VSVG*) were processed for detection of M protein using an anti-tag antibody. The TGN was detected by using an anti-TGN46 (A), and the ER was detected by using an anti-CRT antibody (B). The plasma membrane was labeled by co-expression of CD4 fused to GFP together with the M protein (C). Bars, 20  $\mu$ m. Pearson's correlation coefficients were calculated for each combination of co-staining (D). Error bars, S.E.

between *MΔ20-VSVG* and TGN46 was also strongly decreased ( $0.331 \pm 0.025$ ); however, the *MΔ20-VSVG* protein presented a strong increase of the PCC for CD4 ( $0.79 \pm 0.016$ ) and a mod-

erate increase of the PCC for CRT ( $0.475 \pm 0.018$ ). These results suggest that important intracellular trafficking motifs are present in the distal part of the C-terminal domain of

**Figure 1.** A, schematic drawing of the MERS-M protein with the sequence of residues 149–219 of the C-terminal domain. B and C, subcellular localization of the MERS-CoV M protein. Cells expressing HA-tagged M protein in combination with the GFP-CI-MPR, ERGIC-53-GFP, or CD4 fused with GFP were labeled with an anti-HA antibody. GFP-CI-MPR is a TGN marker, ERGIC-53-GFP is an ER–Golgi intermediate compartment marker, and CD4 is a protein expressed at the cell surface. To detect the ER compartment or the TGN, cells were double-labeled for HA and CRT or TGN46, as indicated. Bars, 20  $\mu$ m. Pearson's correlation coefficients were calculated for each combination of co-staining. D and E, N-terminal or C-terminal added tags have no effect on the TGN localization of the M protein. Cells expressing untagged M protein (M), N- or C-terminally V5-tagged M protein (*V5-M* and *M-V5* respectively), N-terminally HA-tagged M (*HA-M*), or C-terminally VSVG-tagged M (*M-VSVG*) were double-labeled with anti-M antibody together with an anti-TGN46 antibody. Pearson's correlation coefficients were calculated. Error bars, S.E.

## MERS-CoV M protein TGN localization

MERS-CoV M. Analysis of the sequence of the last 20 residues showed that the deleted sequence contains a potential diacidic ER export signal at positions 211–213 (<sup>211</sup>DIE<sup>213</sup>). This signal was first characterized for the glycoprotein of VSV and is indeed present in the VSVG tag (YTDIEMNRLGK) used in our experiments. It is likely that a blockade of ER export arose from the deletion in HA-M $\Delta$ 20 and the loss of the DxE signal; however, the addition of the VSVG tag in the M $\Delta$ 20-VSVG protein restored the signal and rescued the ER export. Moreover, the M $\Delta$ 20-VSVG protein was mainly located at the cell surface instead of being retained in TGN, suggesting that the distal part of the C-terminal domain of the M protein also contains a determinant responsible for its localization in the TGN.

### DxE is a functional ER export signal for MERS-CoV M

To confirm the role of the DxE signal in the ER export of the MERS-M protein, we mutated the aspartic acid and glutamic acid into alanine (D211A/E213A) in the M protein fused with an N-terminal HA tag (HA-M-DxE) or with a C-terminal VSVG tag (M-DxE-VSVG) and analyzed the subcellular localization of the mutants in confocal microscopy. Similarly to HA-M $\Delta$ 20, HA-M-DxE was mainly localized in the ER, whereas M-DxE-VSVG was localized in the TGN (Fig. 2, A and B), confirming that the VSVG tag is able to compensate the D211A/E213A mutation. This result demonstrates that the DxE signal present in the C-terminal domain of MERS-CoV M protein is a functional ER export signal involved in the trafficking of the protein.

### Four residues in the C-terminal domain mediate MERS-CoV M localization to the TGN

The presence of the DxE signal explained the exit of the M protein from the ER but not its retention in the *trans*-Golgi, because it is commonly accepted that in nonpolarized cells, the constitutive secretory pathway leads to the plasma membrane by default (*i.e.* in absence of specific addressing/retention signals). Considering that and the fact that the M $\Delta$ 20-VSVG protein migrates to the cell surface, we looked for the presence of another signal in the last 20 amino acids of the cytosolic tail, which could be involved in the retention of MERS-CoV M in the TGN compartment. For this purpose, we constructed three smaller C-terminal deletion mutants lacking 5, 10, or 15 residues but keeping the VSVG tag to rescue the ER export. These mutants were called M $\Delta$ 5, M $\Delta$ 10, and M $\Delta$ 15. We then compared the subcellular localization of these mutants with the WT and M $\Delta$ 20 M proteins (Fig. 3, A–C). Similar to what was observed for the WT M and in contrast to M $\Delta$ 20 protein, the M $\Delta$ 5, M $\Delta$ 10, and M $\Delta$ 15 proteins co-localized with the TGN46 marker, indicating that the 5-amino acid sequence AGNYR, located between the  $\Delta$ 20 and  $\Delta$ 15 deletions, is likely involved in the specific localization of the protein in the TGN. To identify the residues involved in the TGN localization of the protein, each amino acid (except the alanine) was mutated individually into alanine in the M $\Delta$ 15 protein. M $\Delta$ 15-G201A, M $\Delta$ 15-N202A, M $\Delta$ 15-Y203A, and M $\Delta$ 15-R204A were expressed in HeLa cells, and the subcellular localization of the proteins was analyzed by fluorescence microscopy (Fig. 4). The proteins carrying the mutation G201A, Y203A, or R204A showed a reduced

colocalization with the TGN46 marker compared with the M $\Delta$ 15 (Fig. 4, A and C), with partial export of the protein to the cell surface (Fig. 4, B and C). This difference in intracellular trafficking is illustrated by a decrease of PCC between the M mutants and TGN46 associated with an increase of the PCC with CD4. These results indicate a role of these three residues in the localization of the protein in the TGN. The mutation N202A had no effect on the subcellular localization of the protein compared with the WT. To confirm these results, the mutation G201A, Y203A, or R204A was also inserted into the full-length protein. Analysis of the subcellular localization of these mutants is shown in Fig. 5. M-G201A, M-Y203A, and M-R204A showed a reduced co-localization with TGN46 compared with the WT M-VSVG and an increase of cell surface expression, resulting in an increase of the PCC between the mutant and CD4. To ensure that we identified the full motif involved in the TGN localization of the protein, we also mutated three conserved residues (Tyr-195, Arg-197, or Lys-199) among the betacoronaviruses located upstream of the  $\Delta$ 20 deletion. Interestingly, mutation of the residue Lys-199 also resulted in an increase of the cell surface expression of the protein (Fig. 5).

We also constructed a quadruple mutant protein, M-K199A/G201A/Y203A/R204A (M-KGYR). The extent of colocalization of the quadruple mutant (M-KGYR) with TGN46 and CD4 was in the same range than those of the single mutants.

To confirm the cell surface expression of the M protein when the residues Lys-199, Gly-201, Tyr-203, and Arg-204 are mutated, we performed a cell surface biotinylation assay. The MERS-M protein contains an *N*-glycosylation site in its N-terminal domain (MSNMTQLTE); consequently, the migration profile of the MERS-M protein in immunoblotting renders the quantification of the protein amount difficult (see Fig. 6C), so we also mutated the *N*-glycosylation site in the different mutants. First, we verified that introducing the mutation N3Q had no effect on the intracellular localization of the different proteins (M, M $\Delta$ 20, M-DxE, M-K199A, M-G201A, M-Y203A, M-R204A, and M-KGYR; data not shown). Plasma membrane proteins in cells expressing the different mutants were labeled with nonpermeable biotin, and then biotinylated proteins were precipitated with streptavidin-conjugated agarose beads and analyzed by immunoblotting (Fig. 6, A and B). The M protein is only weakly expressed at the cell surface, with less than 1% of the total amount of protein expression at the cell surface. Mutation of the residues Lys-199, Gly-201, Tyr-203, and Arg-204 alone or in combination induced an increase in cell surface detection of the M protein, with  $\sim$ 13% of the total amount of N3Q-M-KGYR located at the cell surface. Single mutations induced only moderate increases of the cell surface expression compared with the quadruple mutant. The N3Q-M-DxE was barely detected at the cell surface. As seen in an immunofluorescent colocalization assay (Fig. 6B), the expression of the N3Q-M $\Delta$ 20 mutant at the cell surface was slightly increased compared with the WT protein. Together, these results indicated that the residues Lys-199, Gly-201, Tyr-203, and Arg-204 of MERS-CoV M are involved in its specific localization in the TGN.

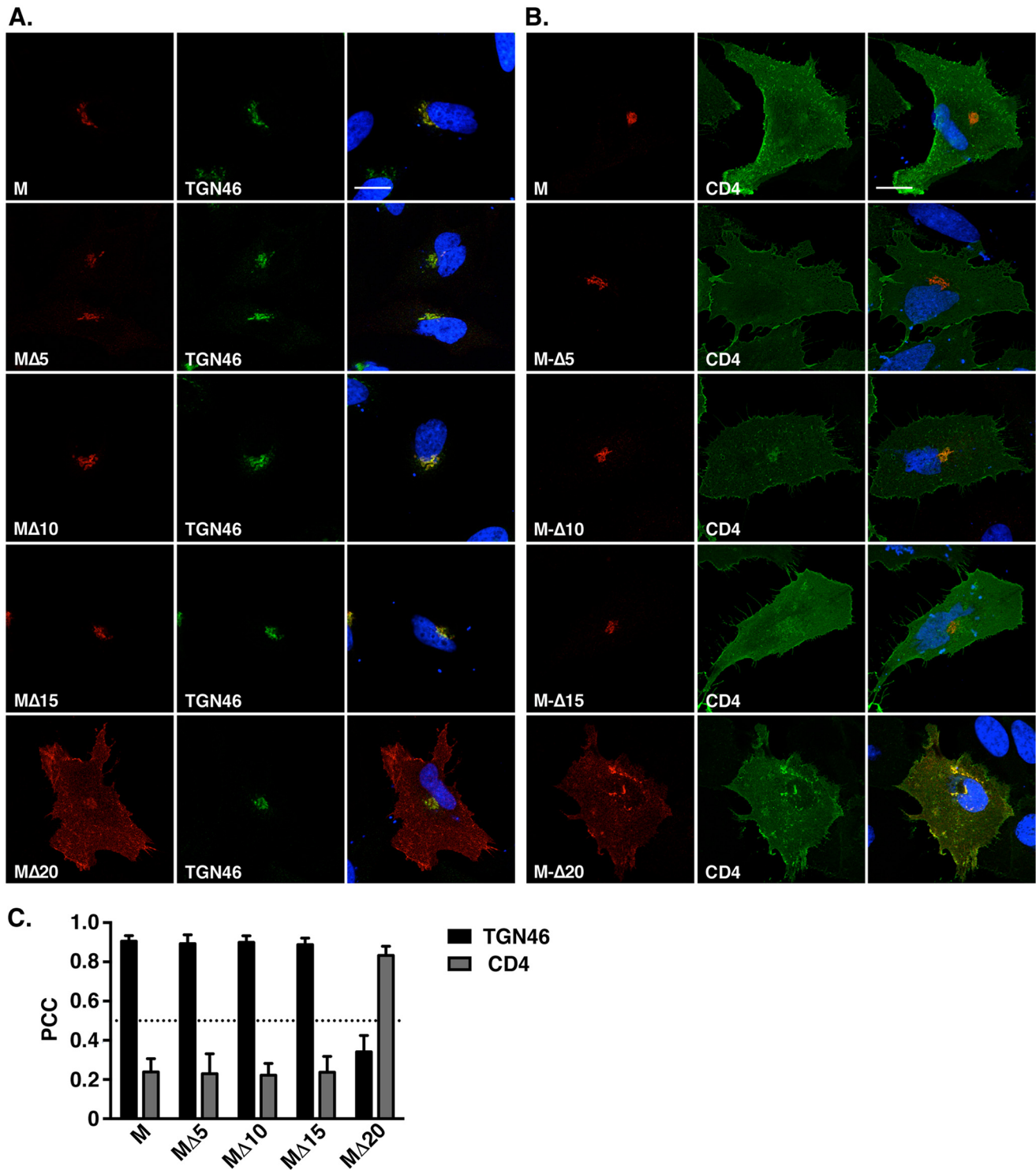
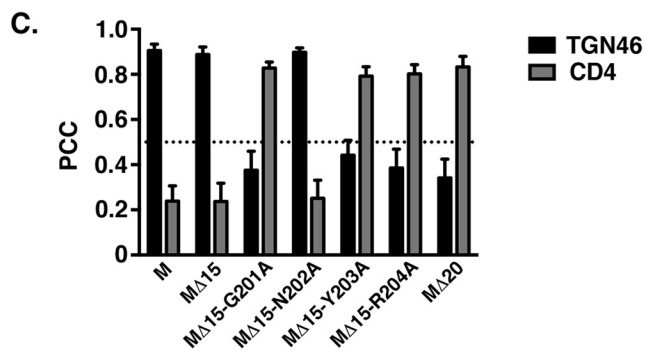
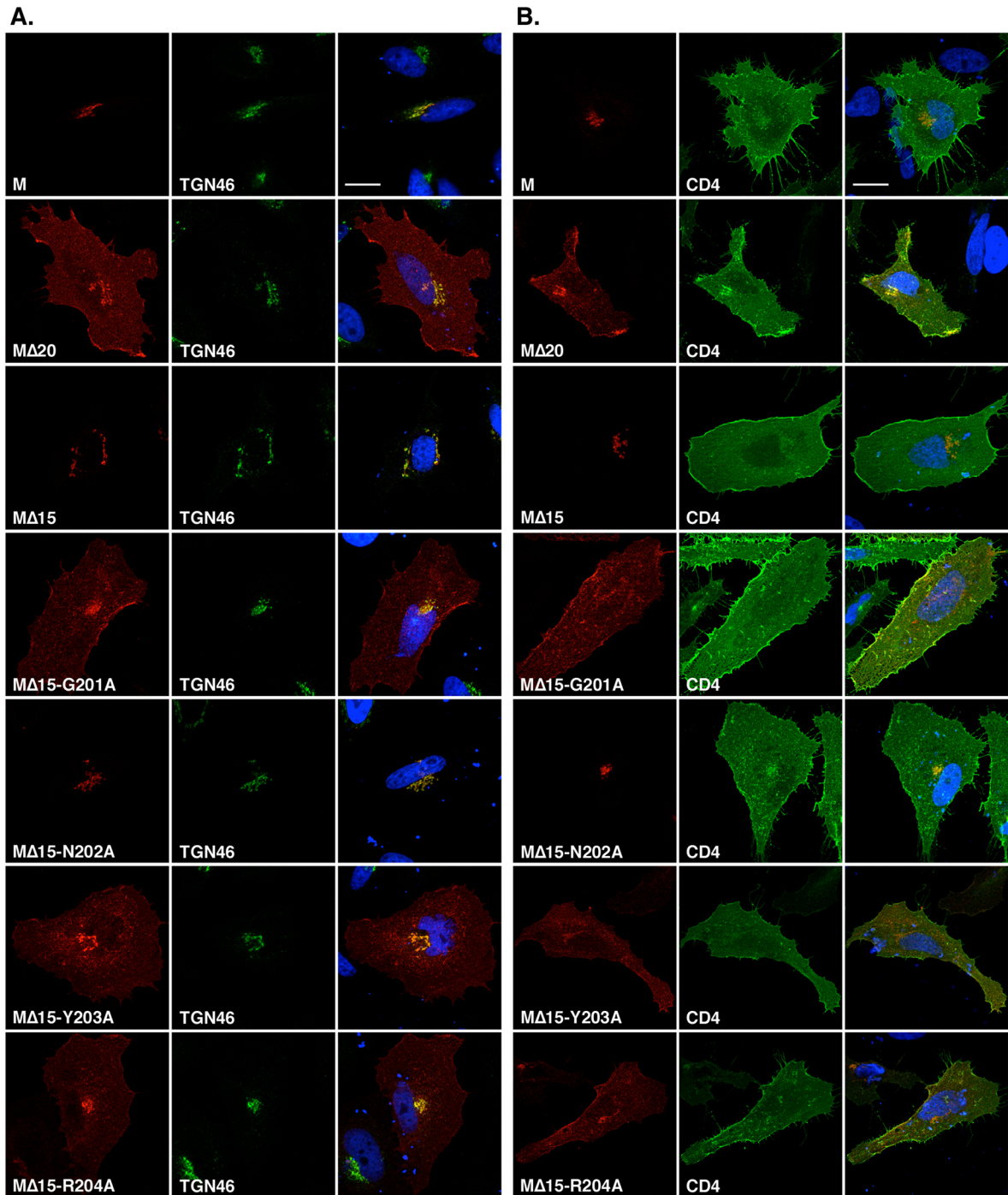


**Figure 3. Subcellular localization of mutants with serial deletions of the distal part of the MERS-CoV M protein.** M protein with a C-terminal VSVG tag (M) or M protein deleted of 5 (M $\Delta$ 5), 10 (M $\Delta$ 10), 15 (M $\Delta$ 15), or 20 amino acid residues (M $\Delta$ 20) was expressed in HeLa cells, and its localization either in the TGN or at the plasma membrane was investigated by double labeling with TGN46 (A) or by co-expressing CD4 fused to GFP (B). Bars, 20  $\mu$ m. Pearson's correlation coefficients were calculated for each combination of co-staining (C). Error bars, S.E.

We also investigated the *N*-glycosylation status of the DxE and KxGxYR mutants. In the immunoblot, the WT protein migrated as three bands (Fig. 6C). A first band of around 20–25 kDa corresponds to the unglycosylated M protein, confirmed by the migration profile of the protein in which the *N*-glycosylation site was abolished by mutation (N3Q-M) and by treat-

ment with PNGase F. A second band of  $\sim$ 30 kDa and a third more diffuse band migrating more slowly were also observed. As expected, the second band is sensitive to endoglycosidase H (EndoH) treatment, showing that this band corresponds to M proteins glycosylated in the ER that have not reached the Golgi yet. The more diffuse band was not sensitive to EndoH treat-

MERS-CoV M protein TGN localization



ment, suggesting that this form is further modified in the Golgi. Only one band was observed with the DxE mutant with a high intensity at 30 kDa sensitive to EndoH. The EndoH sensitivity of the 30 kDa band likely reflects the accumulation of this protein in the ER due to the lack of export signal. It is worth noticing that the migration profile of the M-KGYR mutant in Western blotting showed an increased *N*-glycosylation consistent with a better trafficking through the Golgi (Fig. 6C). Altogether, these results confirm the presence of two intracellular trafficking motifs in the C-terminal domain of the MERS-CoV M protein: first the DxE motif is responsible for the ER export of the protein, and then a second motif, KxGxYR, is involved in its retention in the TGN.

#### **KxGxYR is a not an internalization signal and is not involved in M oligomerization**

Intracellular trafficking is a dynamic process with proteins that can undergo cycles of cell surface expression and internalization. At steady state, the localization of proteins at the plasma membrane results from an equilibrium between anterograde intracellular trafficking and retrieval of protein by endocytosis. Any inhibition of endocytosis would result in protein accumulation at the cell surface. To test whether the KxGxYR motif is an endocytosis signal, we analyzed the endocytosis of the M protein in a biotinylation assay. Proteins expressed at the plasma membrane of cells expressing N3Q-M or N3Q-M-KGYR were labeled at 4 °C with a nonpermeable cleavable biotin, and then endocytosis was allowed by incubating the cells at 37 °C for 30 min. Noninternalized biotin was then cleaved with GSH, and internalized proteins were detected by immunoblotting. As shown in Fig. 6 (E and F), we did not detect any difference in endocytosis levels between the WT protein and M-KGYR.

It has been proposed that oligomerization of MHV-M protein could be involved in its TGN retention. Indeed, mutants that do not form oligomers were detected at the cell surface. In cell lysates, the mutant N3Q-M-KGYR forms dimer in amounts comparable with the WT protein (Fig. 6D). We also analyzed the formation of N3Q-M-KGYR oligomers at the cell surface. To do so, the cell proteins at the cell surface were biotinylated and cross-linked. The formation of multimers was detected by immunoblotting (Fig. 6D). As previously shown, expression of N3Q-M-KGYR at the cell surface was increased. We detected the formation of dimers with a strong band migrating at 40 kDa and also the formation of higher oligomers for both proteins, suggesting that the increased cell surface expression conferred by the mutation of the motif KxGxYR is not due to a defect in M–M interactions. These results indicate that the KxGxYR signal is not involved in M oligomerization and is not an internalization signal and that the localization of MERS-CoV M in the TGN is likely due to a mechanism of retention, preventing the cell surface expression of the protein.

#### **IBV C-terminal domain is involved in its ERGIC localization**

To confirm the role of the KxGxYR as a retention signal in the TGN, we tried to transfer this signal on a protein expressed at the cell surface. We used CD4 as a reporter; however, the chimeric proteins that were constructed presented folding defects (data not shown). CD4 is a type-I transmembrane protein, whereas the M protein has a very different architecture with three transmembrane segments. Therefore, we constructed chimeras between MERS-CoV M and the M protein of another coronavirus, IBV. This way, we were able to construct chimeras that conserved the transmembrane domain structure of the protein, which is likely important for the folding and localization of the protein. The IBV-M protein expressed alone in cells is located in the ERGIC and *cis*-Golgi (26), so its localization can be distinguished from that of MERS-CoV M, using specific compartment markers. In addition, it has been shown that the first transmembrane segment of IBV-M is involved in the intracellular retention of the protein. The amino acid sequences of the MERS- and IBV-M C-terminal extremity are not conserved and are rather different (Fig. 7A).

First, we constructed chimeras in which we switched the C-terminal domains of the proteins: MERS-M/IBV-M and IBV-M/MERS-M or IBV-M/MERS-M-KGYR. We also replaced the first transmembrane segment of the MERS-M-KGYR with that of IBV-M to test whether the first transmembrane segment of IBV-M can retain MERS-M-KGYR intracellularly (TM1-IBV/MERS-M-KGYR). Finally, we replaced the first transmembrane segment of IBV-M with that of MERS-CoV M. Schematic drawings of the different chimeras that were constructed are presented in Fig. 7B. The subcellular localization of the chimeric proteins was then analyzed by fluorescence microscopy. As shown in Fig. 8, the immunofluorescent staining of IBV-M and MERS-CoV M differed in their pattern, with a compact perinuclear staining for MERS-CoV M and a punctuated staining for IBV-M. Co-localization assessment of IBV-M with TGN46 and ERGIC-53 showed that the protein mainly localizes within the ERGIC. The MERS-M/IBV-M protein colocalized with the ERGIC-53 marker and not the TGN46 marker, and is thus located in the ERGIC (Fig. 8C), whereas the IBV-M/MERS-M protein colocalized with the TGN46 marker and not with the ERGIC-53 marker and is thus localized in the TGN. In other words, the switch of the C-terminal domains of the IBV-M and MERS-CoV M proteins caused a switch of their specific localizations, to the ERGIC and the TGN, respectively. Interestingly, the IBV-M/MERS-KGYR protein localized to the cell surface, confirming the role of the KxGxYR signal in the specific localization of the MERS-M protein to the TGN. This result also suggests that the first transmembrane segment of IBV-M is not able to retain MERS-M-KGYR intracellularly. In accordance with this result, the chimera TM1-IBV/MERS-M-KGYR was also located at the cell surface, and the chimera TM1-MERS/IBV-M was located in the ERGIC compartment. These results are unexpected based on previous reports on the role of the first

**Figure 4. Identification of the MERS-CoV M $\Delta$ 15 motif involved in its TGN localization.** Amino acid residues Gly-201, Asn-202, Tyr-203, and Arg-204 located in the last 5 residues of M $\Delta$ 15 (located in the TGN) were mutated individually into alanine, and the subcellular localization of the mutants was analyzed as described in the legend to Fig. 3. Bars, 20  $\mu$ m. Error bars, S.E.

MERS-CoV M protein TGN localization

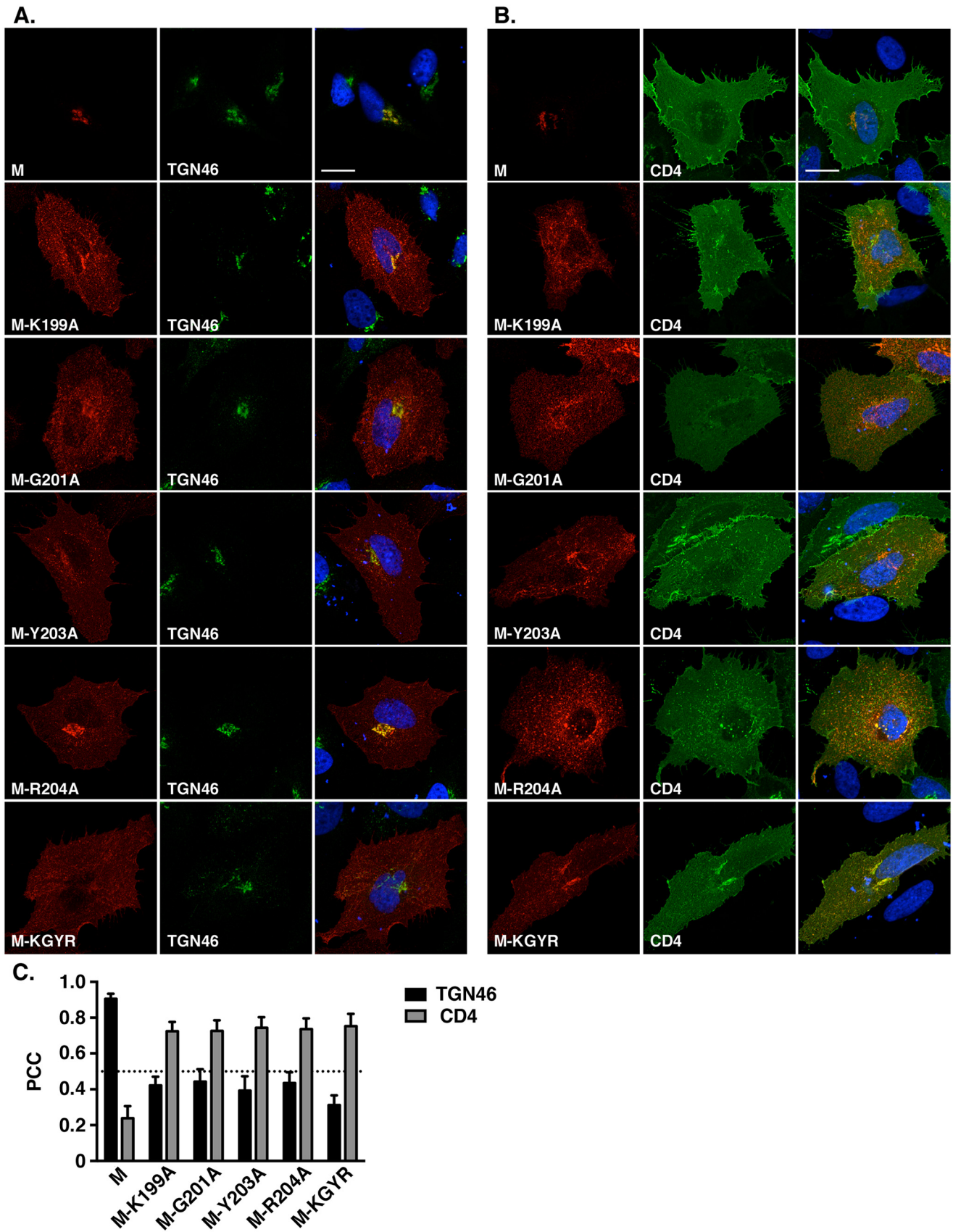


**Figure 5. The KxGxYR motif is involved in MERS-M protein localization in TGN.** The mutations K199A, G201A, Y203A, and R204A were introduced individually or together in the context of the full-length M protein with a C-terminal VSVG tag. The subcellular localization of the mutants was analyzed as described in the legend to Fig. 3. Bars, 20  $\mu$ m. Error bars, S.E.

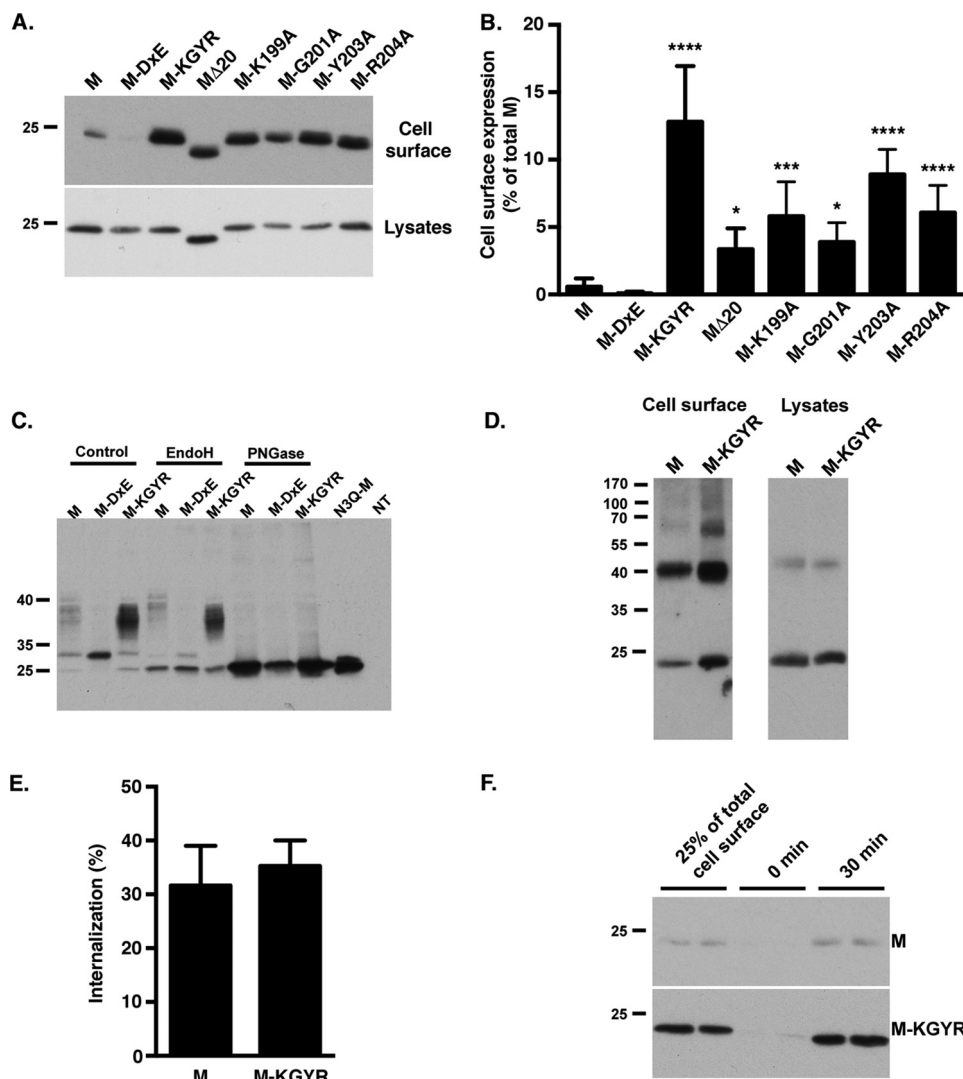


**Figure 6. Cell surface expression of M protein mutants.** Plasma membrane proteins of cells expressing the different M protein mutants were labeled with nonpermeable biotin. Biotinylated proteins were purified using streptavidin-conjugated agarose beads. Biotinylated M proteins and total M proteins in cell lysates were detected by immunoblotting (A) and quantified (B). Results are expressed as the percentage of total M protein expressed at the cell surface and are expressed as the mean of five independent experiments. Error bars, S.E. Results were analyzed by using an analysis of variance test (\*,  $p < 0.1$ ; \*\*,  $p < 0.01$ ; \*\*\*,  $p < 0.001$ ; \*\*\*\*,  $p < 0.0001$ ). Glycosylation of M protein mutants is shown. Lysates of cells expressing the M protein or the M protein with the ER export signal mutated (*M-DxE*) or the TGN localization motif mutated (*M-KGYR*) were treated with EndoH or PNGase F. A lysate of cells expressing the M protein with its N-glycosylation site mutated (N3Q) was left untreated. N-terminal tagged proteins were detected by Western blotting with an anti-V5 antibody (C). Endocytosis of M protein and M-KGYR. Cells were transfected with vectors expressing the M and M-K199A-G210A-Y203A-R204A (*M-KGYR*) proteins. Then cell surface proteins were labeled with nonpermeable biotin at 4 °C. Endocytosis was allowed by incubating the cells for 30 min at 37 °C. Biotin of noninternalized proteins was cleaved with GSH. Internalized M protein was detected after purification with streptavidin-conjugated agarose beads by immunoblotting (E). In each experiment, each condition was performed in duplicate. For cell surface-associated protein, only 25% of the sample was loaded on the gel. For the controls of GSH cleavage (without any internalization, 0 min) and for the samples internalized (30 min), the totality of the samples were loaded on the gel. Internalized M protein was quantified. The results are expressed as the percentage of cell surface-associated M protein and are expressed as the mean of three independent experiments. Error bars, S.E. (E and F).

transmembrane segment of IBV-M in its intracellular retention. Moreover, these results indicate that for both MERS-CoV M and IBV-M, the presence of the C-terminal domain is critical to induce the specific localization of the protein. Furthermore, we also confirmed the involvement of the KxGxYR signal in the specific retention of MERS-CoV M to the TGN, even in the chimeric context.

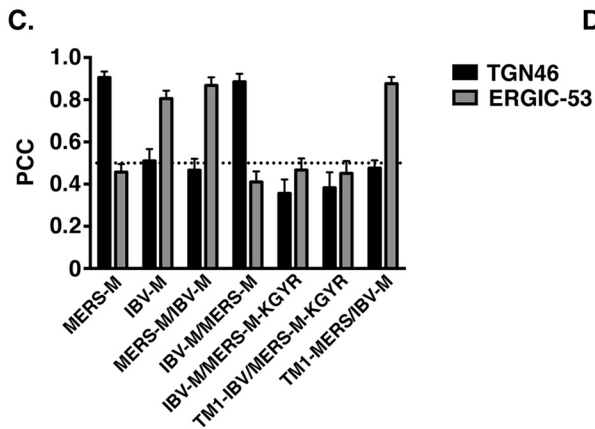
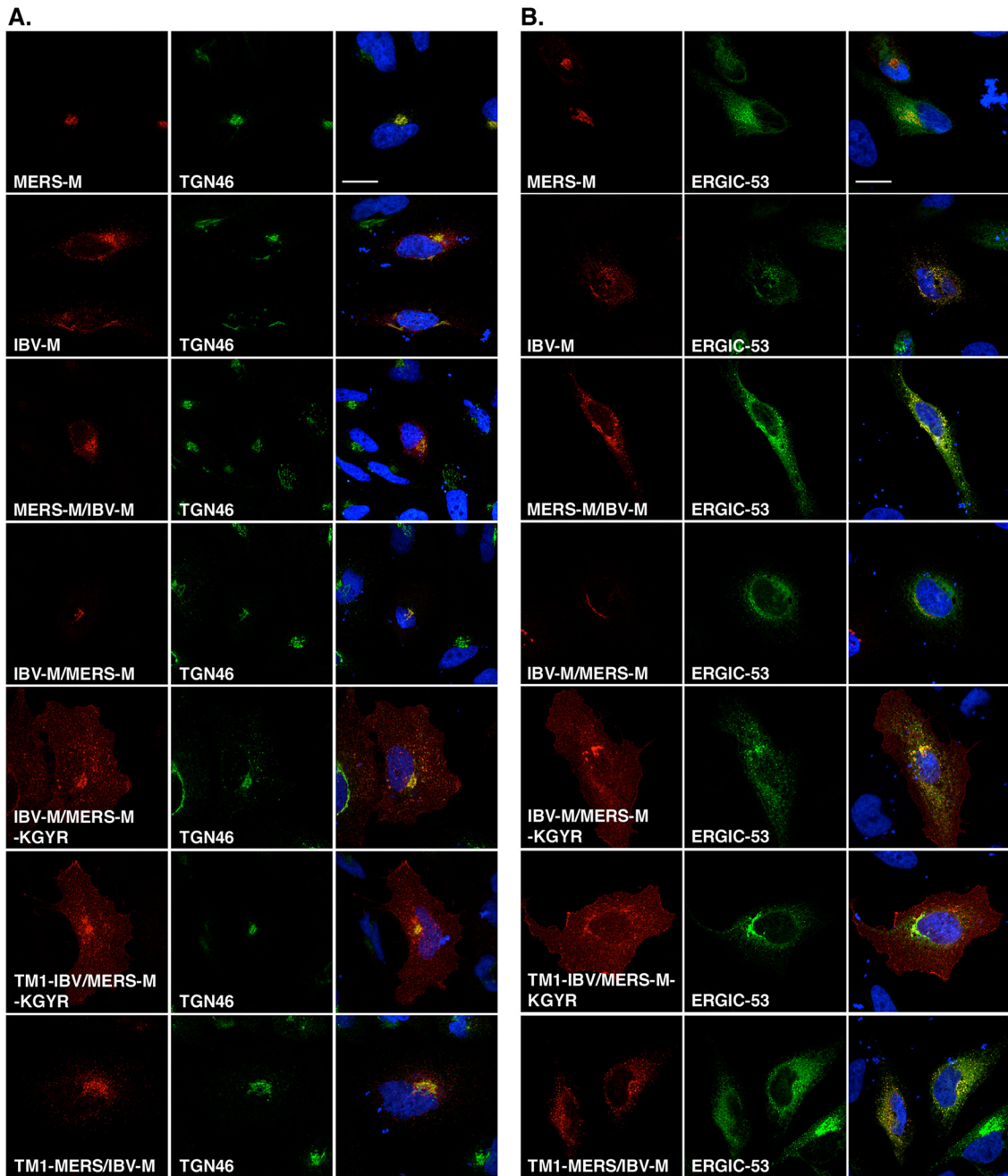
## Discussion

Viruses divert the intracellular trafficking machinery, and studying the intracellular trafficking of viral membrane proteins often helps to decipher the mechanisms of protein sorting

and leads to uncovering new sorting motifs. We investigated the intracellular trafficking of the MERS-CoV M protein and identified a well-known ER export signal. In addition, we identified a novel TGN retention motif.

Specific targeting of viral structural proteins to the assembly site in the cell is crucial for viral egress and spreading. The three envelope proteins of coronaviruses E, M, and S are synthesized in the ER. Protein exit from the ER toward the Golgi occurs at specific sites called ER exit sites and for most of the proteins relies on the coat protein complex II (COPII). Assembly of the coat starts with the activation of the GTPase Sar1 by Sec12, an integral ER guanine nucleotide exchange factor. This allows the





## MERS-CoV M protein TGN localization

their mutants containing a mutation of the KxGxYR motif (Y211G) leaked to the cell surface. These data suggest that TGN localization of M proteins may be a general feature of the beta-coronaviruses and that the KxGxYR motif is involved in this localization. It has been reported that the SARS-CoV M protein is located in the Golgi; unfortunately, its precise localization within the Golgi remains unclear (37, 38).

Locker *et al.* (39) reported that oligomerization of MHV-M protein is involved in the TGN retention of the protein; however, our results show that it is unlikely that the KxGxYR motif is involved in the oligomerization of the protein. As a small proportion of the MERS-CoV M protein could be detected at the cell surface (less than 1% of the total protein; see Fig. 6, A and B), we tested whether the KxGxYR motif could be an endocytosis motif. The MERS-CoV M protein is retrieved from the cell surface by endocytosis; however, we could not detect any defect of endocytosis of the M protein when the KxGxYR motif was mutated (Fig. 6, E and F). This result argues against an endocytic function of this motif and suggests a role as a retention signal. Indeed, it was reported previously (27) that the MHV-M protein does not cycle between the plasma membrane of the cell and the TGN but rather acts as a TGN-resident protein. Another hypothesis is a cycle of the M between the ER and the TGN with the KxGxYR motif acting as a retrieval signal from the TGN to the ER. The mutation of this signal would inhibit the retrieval of the protein, allowing its trafficking to the cell surface. The retrograde trafficking ensures the constant recycling of proteins and lipids from the Golgi to the ER to maintain their steady-state distribution and the composition and function of the organelles themselves. Two distinct mechanisms are responsible for this retrograde transport. The first one depends on the coat protein complex I (COPI), and the second one is the COPI-independent pathway that is less characterized, involves the Rab6 GTPase, and is composed of tubular rather than vesicular carriers (40). The formation of the COPI-coated vesicles starts with the recruitment en bloc of the coatomer composed of seven subunits by the Arf1 GTPase. Cargos carry specific signals in their cytosolic-exposed domain mediating their recruitment by COPI. The best characterized motifs are the di-lysine motifs KKxx or KxKxx that are recognized by the  $\alpha$ -COP or  $\beta'$ -COP subunit of the coatomer. Multimeric proteins, such as receptors or channels, contain an arginine-based sorting signal ( $\phi$ RxR, where  $\phi$  represents any hydrophobic amino acid). A common feature of the motif involved in the protein sorting toward the COPI-dependent pathway is the presence of basic residues. Because of its content in basic residues, the KxGxYR motif might be recognized by the COPI machinery to prevent its cell surface expression.

Nevertheless, the mechanism of action of the KxGxYR motif remains to be further elucidated, particularly in the context of the viral infection. Indeed, the retention of the protein may be important for the proper assembly of the viral particle by promoting interaction with the other viral membrane components. How the interaction with E or S may mask the KxGxYR reten-

tion signal or how these protein complexes may further traffic through the biosynthetic pathway remains to be clarified.

Furthermore, we cannot exclude the possibility that other domains of the protein may also be implicated in the TGN localization of the protein. As mentioned above, the transmembrane domain and an endocytic motif cooperate for the proper localization of TGN38/46. The Golgi apparatus is a compartmentalized structure where glycosylation occurs in an ordered process (41). The successful completion of glycosylation relies in part on the proper distribution of glycosyltransferases along the Golgi that will permit their action in a sequential manner. Most of the glycosyltransferases are type II transmembrane proteins. They consist of a short N-terminal domain exposed in the cytosol, a transmembrane domain, a stem region, and an enzymatic domain. The nonuniform distribution of these enzymes in the Golgi is likely maintained by a combination of retention and recycling mechanisms (42). The mechanisms that ensure the localization of glycosyltransferases in the Golgi are numerous and diverse. These include the oligomerization status of the enzyme and complex formation, the length of the transmembrane domain but also its composition, which may affect the way it is interacting with the different lipid compositions that the protein encounters in the different Golgi cisternae. The cytosolic domains also contain motifs involved in the localization of the enzymes (42).

To confirm the role of the KxGxYR motif as a retention signal in the TGN, we attempted to transfer the motif in CD4, a protein expressed at the plasma membrane. Unfortunately, the different chimeras that we constructed were not folded properly. This was likely due to the difference of protein structures, CD4 being a type I transmembrane protein, whereas MERS-CoV M is a triple membrane-spanning protein. Therefore, to further confirm the role of the KxGxYR motif, we constructed chimeras between MERS-CoV M and IBV-M, as they show clear differences in subcellular localization at steady state. Indeed, IBV-M is mainly expressed in the ERGIC and *cis*-Golgi compartment. Previous studies reported the role of the first transmembrane segment in the intracellular retention of the protein (26). This was shown by the replacement of the transmembrane domain of the glycoprotein G of the vesicular stomatitis virus (VSVG) with the first transmembrane segment of IBV-M, which resulted in the intracellular retention of the protein, and four polar residues were shown to mediate this retention (25). Surprisingly, when we replaced the first membrane-spanning domain of MERS-CoV M with that of IBV-M in the context where the KxGxYR motif is mutated into alanine residues (TM1-IBV/MERS-M-KGYR), the protein was not located in the ERGIC but was still transported to the cell surface. This difference may lie in the use of a full-length coronavirus M protein instead of a reporter protein such as VSVG. Interestingly, when we swapped the C-terminal domains of the proteins, we also switched their specific localizations, suggesting that the IBV-M C-terminal domain contains a signal(s) for the

**Figure 8. Subcellular localization of IBV-M and MERS-CoV M proteins chimeras.** The localization of the different chimeras in the TGN or in the ERGIC compartments was investigated by immunofluorescent double labeling by using an anti-VSVG antibody and an anti-TGN46 (A) or by expressing the ERGIC-53 marker conjugated with GFP (B). Bars, 20  $\mu$ m. Pearson's correlation coefficients were calculated for each combination of co-staining (C). Error bars, S.E.

ERGIC localization of the protein and not the first membrane segment as reported previously.

Altogether, our results suggest that the C-terminal domain of coronavirus M proteins dictates their specific localization, the betacoronavirus M proteins being addressed to the TGN, where they are retained by the action of the KxGxYR motif. The motif mediating IBV-M localization in the ERGIC and *cis*-Golgi compartment remains, however, to be determined. At this state of knowledge, we cannot exclude the possibility that the membrane-spanning segments of the protein additionally participate in the intracellular retention of these proteins and cooperate with the C-terminal domain to prevent the expression of the protein at the cell surface.

## Experimental procedures

### Plasmids

The coding sequence of the M protein was cloned in the pCDNA3.1(+) vector, with or without a sequence coding for different tags, including HA, VSVG, and V5. Total RNA from blood samples of an infected patient were extracted by using the Nucleospin RNA kit (Macherey-Nagel) according to the manufacturer's instructions. Then reverse transcription was performed using the high-capacity cDNA reverse transcription kit (Applied Biosystems), and the M protein sequence was amplified by two successive PCRs. First, the sequence was amplified by using the two following primers: 5'-gacgagtgggttaacgaact-3' and 5'-ggggatgccataacaatgaaa-3'. Then, to insert the sequence in expression vectors, the sequence was amplified with 5'-tcggatccaccatgctctaataatgacgcaactcactg-3' (primer A) and 5'cagaattcctaagctcgaagcaatgcaa-3' (primer B; untagged protein) or by combination of primer A and 5'-tagaattcagctcgaagcaatgcaagtcaat-3' (primer C; C-terminal tagged protein) or with 5'-acggatccaatgacgcaactcactgagg-3' (primer D) with primer B (N-terminal tagged protein). PCR products were inserted between the BamHI and EcoRI restriction sites of the different vectors.

M protein deletion mutants were generated by PCR by using either primer A or D in combination with a reverse primer annealing at different positions of the M sequence, with or without a stop codon with an EcoRI restriction site. M protein point mutants were generated by site-directed mutagenesis using PCR. Overlapping primers containing the mutation(s) of interest were designed and used for PCR on a MERS-M WT template. PCRs were then gel-purified, digested, and cloned into a pCDNA3.1-VSVG or pCDNA3.1-HA plasmid. The chimeric constructions were generated by fusion PCR. For IBV-M/MERS-M-Ct, the sequence of IBV-M corresponding to residues 1–101 were amplified with the forward primer 5'-ttaagctttccatgcccaacgagacaaattg-3' and the reverse primer 5'-taaacagccgaataactctggatccaataac-3', containing 10 bases complementary to the MERS-M sequence at its 5' extremity. The MERS-M sequence between residues 100 and 219 was amplified by PCR using the forward primer 5'-ccagagtATTcg-gctgtttatgagaactgg-3' containing 10 bases complementary to the IBV-M sequence and with the primer D. Then the two PCR products were mixed and amplified using the forward primer that anneals the IBV-M sequence and the primer D. Using the

same strategy of overlapping sequences for the internal primers, we constructed MERS-M/IBV-M-Ct composed of the MERS-M<sub>1–102</sub> fused to IBV-M<sub>105–225</sub>. The first transmembrane segment of the MERS-M-KGYR was replaced by the first transmembrane segment of IBV-M by fusing IBV-M<sub>1–42</sub> to MERS-M-KGYR<sub>41–219</sub> (TM1-IBV/MERS-M-KGYR), and the first transmembrane segment of IBV-M was replaced by the first transmembrane segment of MERS-M by fusing MERS-M<sub>1–40</sub> to IBV-M<sub>43–225</sub> (TM1-MERS/IBV-M). The PCR products were gel-purified and digested by BamHI and EcoRI and then inserted into the pCDNA3.1-V5 expression vector. All of the constructs were verified by DNA sequencing.

The plasmids coding the ERGIC-53 protein fused to the GFP and coding the GFP-CI-MPR were kindly provided by Dr. Hauri (University of Basel) and Dr. Hoflack (University of Dresden) respectively. The plasmid encoding the CD4-GFP fusion protein was constructed by amplification of the GFP with the two primers 5'-AGACATGTAGCCCCATTGTGAGCAAGG-GCGAGGAGCT-3' and 5'-GGGTCGACTCACTTGTACAGCTCGTCCATGC-3' and then inserted into the PCI-CD4 between the AflIII and SalI restriction sites.

### Cell culture and transfection

HeLa cells were maintained in minimal essential medium supplemented with 10% fetal calf serum and 1% Glutamax. 24 h before transfection, HeLa cells were plated in 24-well plates on coverslips or in 6-well plates. The next day, plasmids encoding WT M protein or M mutant protein were transfected into HeLa cells using TransIT<sup>®</sup>-LT1 transfection reagent (Mirus Bio).

### Immunofluorescence and confocal microscopy

At 18 h post-transfection, cells were rinsed with PBS, fixed with 3% PFA, and processed for immunofluorescence analysis. Cells were permeabilized with 0.1% Triton X-100 in PBS for 5 min and then blocked with buffer containing 10% goat or horse serum in PBS for 10 min. M protein was detected using anti-M pAbs (rabbit, Proteogenix) or anti-tag antibodies: anti-HA mAbs (3F10, Sigma-Aldrich), anti-VSVG mAbs (P5D4, produced in the laboratory of the authors), or anti-V5 mAbs (Thermo Fisher Scientific). For co-localization experiments, cells were double-labeled for M-proteins and cellular marker, anti-CRT pAbs for endoplasmic reticulum (ER) and anti-TGN46 pAbs for TGN (Bio-Rad). Primary antibodies were diluted in blocking buffer. In some cases, intracellular compartments were stained by transfecting an expression vector for a marker fused with GFP. For ERGIC and TGN compartments, cells were co-transfected with M proteins and expression vectors for ERGIC53 and M6PR fused to GFP, respectively. For cell surface staining, cells were transfected with a vector expressing CD4 fused to GFP. After a 30-min incubation with primary antibodies, cells were washed three times for 5 min with PBS. Then the cells were incubated with fluorescent secondary antibodies (cyanine-3–conjugated goat anti-mouse IgG; cyanine-3–conjugated goat anti-rabbit IgG; Alexa 488–conjugated donkey anti-rat IgG; cyanine-3–conjugated donkey anti-sheep IgG; Alexa 488–conjugated donkey anti-mouse IgG; Alexa 555–conjugated goat anti-rat IgG) and 1 μg/ml 4',6-diamidino-2-phenylindole.

## MERS-CoV M protein TGN localization

Images were acquired using a laser-scanning confocal microscope LSM 880 (Zeiss) using a  $\times 63$  oil immersion objective. Signals were sequentially collected using single fluorescence excitation and acquisition settings to avoid crossover.

The extent of colocalization was quantified by calculating the PCC using the JACoP plugin of ImageJ. The PCC examines the relationship between the intensities of the pixels of two channels in the same image. For each calculation, at least 15 images were analyzed to obtain a PCC mean. A PCC of 1 indicates perfect correlation, 0 no correlation, and  $-1$  perfect anti-correlation.

### Biotinylation and internalization assay

HeLa cells were seeded in 6-well plates and transfected the next day with pCDNA3.1-V5-N3Q-M, pCDNA3.1-V5-N3Q-M $\Delta$ 20, pCDNA3.1-V5-N3Q-M-D211A,E213A, pCDNA3.1-V5-N3Q-M-K199A,G201A,Y203A,R204A, pCDNA3.1-V5-N3Q-M-K199A, pCDNA3.1-V5-N3Q-M-G201A, pCDNA3.1-V5-N3Q-M-Y203A, or pCDNA3.1-V5-N3Q-M-R204A. At 24 h post-transfection, cells were rinsed on ice with ice-cold PBS and incubated twice with 250  $\mu\text{g/ml}$  EZ-Link<sup>TM</sup> Sulfo-NHS-SS-Biotin (Pierce) diluted in PBS for 15 min to label cell surface proteins. Unfixed biotin was then quenched by two sequential incubations of the cells for 10 min with 50 mM glycine/PBS.

For internalization assays, cells were biotinylated 48 h post-transfection and then incubated at 37 °C for 30 min. The biotin of nonendocytosed proteins was then cleaved upon three incubations of 20 min with GSH buffer (50 mM reduced GSH, 75 mM NaCl, 75 mM NaOH, 10% fetal calf serum) followed by two incubations of 15 min with iodoacetamide buffer (50 mM iodoacetamide, 1% BSA, PBS).

Cells were then lysed with B1 buffer (50 mM Tris, pH 7.5, 100 mM NaCl, 2 mM EDTA, 1% Triton X-100, 0.1% SDS, protease inhibitor mixture) on ice. Lysates were centrifuged at 14,000 rpm at 4 °C for 5 min to remove cellular debris and were then incubated with 30  $\mu\text{l}$  of streptavidin-conjugated agarose beads (Sigma) for 2 h. Beads were then washed serially with 1 ml of buffers B1, B2 (50 mM Tris, pH 7.5, 100 mM NaCl, 2 mM EDTA, 0.1% Triton X-100, 0.5% SDS, 0.5% deoxycholate), B3 (50 mM Tris, pH 7.5, 500 mM NaCl, 2 mM EDTA, 0.1% Triton X-100), and B4 (50 mM Tris, pH 7.5, 100 mM NaCl, 2 mM EDTA). Proteins were resuspended in Laemmli loading buffer and detected by immunoblotting. Samples were separated by SDS-PAGE, and proteins were transferred on a nitrocellulose membrane (Amersham Biosciences). Membrane-bound M proteins were then detected using a monoclonal anti-V5 antibody and horseradish peroxidase-conjugated secondary antibody. Detection was carried out by chemiluminescence (Pierce).

### Glycosidase treatment

HeLa cells were transfected with vectors expressing V5-M, V5-M-DxE, V5-M-KGYR, or V5-N3Q-M proteins. 24 h later, cells were lysed in B1 buffer. Then, 30  $\mu\text{l}$  of lysates were mock-treated or treated with PNGase F or endoglycosidase H according to the manufacturer's instructions. Then proteins were separated on SDS-PAGE and detected by immunoblotting.

### M-M interaction assay

HeLa cells were seeded in 10-cm dishes and transfected with vectors expressing V5-N3Q-M or V5-N3Q-M-KGYR. The next day, cell surface proteins were biotinylated at 4 °C and cross-linked with 0.8% PFA in PBS for 10 min. Then PFA was quenched by washing the cells with 50 mM  $\text{NH}_4\text{Cl}$ /PBS twice. Cells were lysed with B1 buffer, and lysates were processed for streptavidin precipitation as described previously. Proteins were resuspended in nonreducing Laemmli loading buffer without heating and detected by immunoblotting.

*Author contributions*—A. P. and S. B. formal analysis; A. P., A. B., L. D., A. D., and S. B. investigation; A. P., J. D., and S. B. writing-original draft; A. P., A. B., L. D., A. G., Y. R., J. D., and S. B. writing-review and editing; L. D., A. G., Y. R., J. D., and S. B. conceptualization; A. D. and Y. R. resources; J. D. and S. B. supervision; S. B. funding acquisition.

*Acknowledgments*—We thank Hans-Peter Hauri, Bernard Hoflacker, and Gary Whittaker for providing reagents. The immunofluorescence analyses were performed with the help of the imaging core facility of the BioImaging Center Lille Nord-de-France.

### References

1. Masters, P. S. (2006) The molecular biology of coronaviruses. *Adv. Virus Res.* **66**, 193–292 [CrossRef Medline](#)
2. Perlman, S., and Netland, J. (2009) Coronaviruses post-SARS: update on replication and pathogenesis. *Nat. Rev. Microbiol.* **7**, 439–450 [CrossRef Medline](#)
3. Corman, V. M., Muth, D., Niemeyer, D., and Drosten, C. (2018) Hosts and sources of endemic human coronaviruses. *Adv. Virus Res.* **100**, 163–188 [CrossRef Medline](#)
4. Belouzard, S., Millet, J. K., Licitra, B. N., and Whittaker, G. R. (2012) Mechanisms of coronavirus cell entry mediated by the viral spike protein. *Viruses* **4**, 1011–1033 [CrossRef Medline](#)
5. Heald-Sargent, T., and Gallagher, T. (2012) Ready, set, fuse! The coronavirus spike protein and acquisition of fusion competence. *Viruses* **4**, 557–580 [CrossRef Medline](#)
6. Ruch, T. R., and Machamer, C. E. (2012) The coronavirus E protein: assembly and beyond. *Viruses* **4**, 363–382 [CrossRef Medline](#)
7. Nieto-Torres, J. L., Verdía-Báguena, C., Castaño-Rodríguez, C., Aguilera, V. M., and Enjuanes, L. (2015) Relevance of viroporin ion channel activity on viral replication and pathogenesis. *Viruses* **7**, 3552–3573 [CrossRef Medline](#)
8. Westerbeck, J. W., and Machamer, C. E. (2019) The infectious bronchitis coronavirus envelope protein alters Golgi pH to protect spike protein and promote release of infectious virus. *J. Virol.* **93**, e00015-19 [CrossRef Medline](#)
9. Westerbeck, J. W., and Machamer, C. E. (2015) A coronavirus E protein is present in two distinct pools with different effects on assembly and the secretory pathway. *J. Virol.* **89**, 9313–9323 [CrossRef Medline](#)
10. de Haan, C. A. M., and Rottier, P. J. M. (2005) Molecular interactions in the assembly of coronaviruses. *Adv. Virus Res.* **64**, 165–230 [CrossRef Medline](#)
11. de Haan, C. A., Kuo, L., Masters, P. S., Vennema, H., and Rottier, P. J. (1998) Coronavirus particle assembly: primary structure requirements of the membrane protein. *J. Virol.* **72**, 6838–6850 [Medline](#)
12. Opstelten, D. J., Raamsman, M. J., Wolfs, K., Horzinek, M. C., and Rottier, P. J. (1995) Envelope glycoprotein interactions in coronavirus assembly. *J. Cell Biol.* **131**, 339–349 [CrossRef Medline](#)
13. de Haan, C. A., Smeets, M., Vernooij, F., Vennema, H., and Rottier, P. J. (1999) Mapping of the coronavirus membrane protein domains involved in interaction with the spike protein. *J. Virol.* **73**, 7441–7452 [Medline](#)
14. Arndt, A. L., Larson, B. J., and Hogue, B. G. (2010) A conserved domain in the coronavirus membrane protein tail is important for virus assembly. *J. Virol.* **84**, 11418–11428 [CrossRef Medline](#)

15. Tseng, Y.-T., Wang, S.-M., Huang, K.-J., Lee, A. I.-R., Chiang, C.-C., and Wang, C.-T. (2010) Self-assembly of severe acute respiratory syndrome coronavirus membrane protein. *J. Biol. Chem.* **285**, 12862–12872 [CrossRef Medline](#)
16. de Haan, C. A. M., Vennema, H., and Rottier, P. J. M. (2000) Assembly of the coronavirus envelope: homotypic interactions between the M proteins. *J. Virol.* **74**, 4967–4978 [CrossRef Medline](#)
17. Baudoux, P., Carrat, C., Besnardeau, L., Charley, B., and Laude, H. (1998) Coronavirus pseudoparticles formed with recombinant M and E proteins induce  $\alpha$  interferon synthesis by leukocytes. *J. Virol.* **72**, 8636–8643 [Medline](#)
18. Vennema, H., Godeke, G. J., Rossen, J. W., Voorhout, W. F., Horzinek, M. C., Opstelten, D. J., and Rottier, P. J. (1996) Nucleocapsid-independent assembly of coronavirus-like particles by co-expression of viral envelope protein genes. *EMBO J.* **15**, 2020–2028 [CrossRef Medline](#)
19. Lim, K. P., and Liu, D. X. (2001) The missing link in coronavirus assembly: retention of the avian coronavirus infectious bronchitis virus envelope protein in the pre-Golgi compartments and physical interaction between the envelope and membrane proteins. *J. Biol. Chem.* **276**, 17515–17523 [CrossRef Medline](#)
20. Siu, Y. L., Teoh, K. T., Lo, J., Chan, C. M., Kien, F., Escriou, N., Tsao, S. W., Nicholls, J. M., Altmeyer, R., Peiris, J. S. M., Bruzzone, R., and Nal, B. (2008) The M, E, and N structural proteins of the severe acute respiratory syndrome coronavirus are required for efficient assembly, trafficking, and release of virus-like particles. *J. Virol.* **82**, 11318–11330 [CrossRef Medline](#)
21. Klumperman, J., Locker, J. K., Meijer, A., Horzinek, M. C., Geuze, H. J., and Rottier, P. J. (1994) Coronavirus M proteins accumulate in the Golgi complex beyond the site of virion budding. *J. Virol.* **68**, 6523–6534 [Medline](#)
22. Salanueva, I. J., Carrascosa, J. L., and Risco, C. (1999) Structural maturation of the transmissible gastroenteritis coronavirus. *J. Virol.* **73**, 7952–7964 [Medline](#)
23. Machamer, C. E., Mentone, S. A., Rose, J. K., and Farquhar, M. G. (1990) The E1 glycoprotein of an avian coronavirus is targeted to the cis Golgi complex. *Proc. Natl. Acad. Sci. U.S.A.* **87**, 6944–6948 [CrossRef Medline](#)
24. Locker, J. K., Griffiths, G., Horzinek, M. C., and Rottier, P. J. (1992) O-glycosylation of the coronavirus M protein: differential localization of sialyltransferases in N- and O-linked glycosylation. *J. Biol. Chem.* **267**, 14094–14101 [Medline](#)
25. Machamer, C. E., Grim, M. G., Esquela, A., Chung, S. W., Rolls, M., Ryan, K., and Swift, A. M. (1993) Retention of a cis Golgi protein requires polar residues on one face of a predicted  $\alpha$ -helix in the transmembrane domain. *Mol. Biol. Cell* **4**, 695–704 [CrossRef Medline](#)
26. Machamer, C. E., and Rose, J. K. (1987) A specific transmembrane domain of a coronavirus E1 glycoprotein is required for its retention in the Golgi region. *J. Cell Biol.* **105**, 1205–1214 [CrossRef Medline](#)
27. Locker, J. K., Klumperman, J., Oorschot, V., Horzinek, M. C., Geuze, H. J., and Rottier, P. J. (1994) The cytoplasmic tail of mouse hepatitis virus M protein is essential but not sufficient for its retention in the Golgi complex. *J. Biol. Chem.* **269**, 28263–28269 [Medline](#)
28. Waguri, S., Dewitte, F., Le Borgne, R., Rouillé, Y., Uchiyama, Y., Dubremetz, J.-F., and Hoflack, B. (2003) Visualization of TGN to endosome trafficking through fluorescently labeled MPR and AP-1 in living cells. *Mol. Biol. Cell.* **14**, 142–155 [CrossRef Medline](#)
29. Dunn, K. W., Kamocka, M. M., and McDonald, J. H. (2011) A practical guide to evaluating colocalization in biological microscopy. *Am. J. Physiol. Cell Physiol.* **300**, C723–C742 [CrossRef Medline](#)
30. Venditti, R., Wilson, C., and De Matteis, M. A. (2014) Exiting the ER: what we know and what we don't. *Trends Cell Biol.* **24**, 9–18 [CrossRef Medline](#)
31. Geva, Y., and Schuldiner, M. (2014) The back and forth of cargo exit from the endoplasmic reticulum. *Curr. Biol.* **24**, R130–R136 [CrossRef Medline](#)
32. Votsmeier, C., and Gallwitz, D. (2001) An acidic sequence of a putative yeast Golgi membrane protein binds COPII and facilitates ER export. *EMBO J.* **20**, 6742–6750 [CrossRef Medline](#)
33. Yang, Y., Zhang, L., Geng, H., Deng, Y., Huang, B., Guo, Y., Zhao, Z., and Tan, W. (2013) The structural and accessory proteins M, ORF 4a, ORF 4b, and ORF 5 of Middle East respiratory syndrome coronavirus (MERS-CoV) are potent interferon antagonists. *Protein Cell* **4**, 951–961 [CrossRef Medline](#)
34. Bos, K., Wraight, C., and Stanley, K. K. (1993) TGN38 is maintained in the trans-Golgi network by a tyrosine-containing motif in the cytoplasmic domain. *EMBO J.* **12**, 2219–2228 [CrossRef Medline](#)
35. Ponnambalam, S., Rabouille, C., Luzio, J. P., Nilsson, T., and Warren, G. (1994) The TGN38 glycoprotein contains two non-overlapping signals that mediate localization to the trans-Golgi network. *J. Cell Biol.* **125**, 253–268 [CrossRef Medline](#)
36. Armstrong, J., and Patel, S. (1991) The Golgi sorting domain of coronavirus E1 protein. *J. Cell Sci.* **98**, 567–575 [Medline](#)
37. Nal, B., Chan, C., Kien, F., Siu, L., Tse, J., Chu, K., Kam, J., Staropoli, I., Crescenzo-Chaigne, B., Escriou, N., van der Werf, S., Yuen, K. Y., and Altmeyer, R. (2005) Differential maturation and subcellular localization of severe acute respiratory syndrome coronavirus surface proteins S, M and E. *J. Gen. Virol.* **86**, 1423–1434 [CrossRef Medline](#)
38. McBride, C. E., and Machamer, C. E. (2010) A single tyrosine in the severe acute respiratory syndrome coronavirus membrane protein cytoplasmic tail is important for efficient interaction with spike protein. *J. Virol.* **84**, 1891–1901 [CrossRef Medline](#)
39. Locker, J. K., Opstelten, D. J., Ericsson, M., Horzinek, M. C., and Rottier, P. J. (1995) Oligomerization of a trans-Golgi/trans-Golgi network retained protein occurs in the Golgi complex and may be part of its retention. *J. Biol. Chem.* **270**, 8815–8821 [CrossRef Medline](#)
40. Heffernan, L. F., and Simpson, J. C. (2014) The trials and tribulations of Rab6 involvement in Golgi-to-ER retrograde transport. *Biochem. Soc. Trans.* **42**, 1453–1459 [CrossRef Medline](#)
41. Puthenveedu, M. A., and Linstedt, A. D. (2005) Subcompartmentalizing the Golgi apparatus. *Curr. Opin. Cell Biol.* **17**, 369–375 [CrossRef Medline](#)
42. Tu, L., and Banfield, D. K. (2010) Localization of Golgi-resident glycosyltransferases. *Cell. Mol. Life Sci.* **67**, 29–41 [CrossRef Medline](#)